Effect of Organic Peroxides on the Morphology and Properties of EVA/Cloisite 15A Nanocomposites

S. B. Mishra, A. S. Luyt

Department of Chemistry, University of the Free State (Qwaqwa Campus), Phuthaditjhaba 9866, South Africa

Received 5 September 2007; accepted 18 September 2008
DOI 10.1002/app.29400
Published online 22 December 2008 in Wiley InterScience (www.interscience.wiley.com).

ABSTRACT: This article describes the effect of the presence of organic peroxides on the morphology and properties of ethylene vinyl acetate copolymer (EVA)/Cloisite 15A nanocomposites. The results show that the presence of dicumyl peroxide (DCP) or dibenzoyl peroxide (DBP) during the preparation of EVA/Cloisite 15A clay nanocomposites gives rise to intercalated, exfoliated, or mixed morphologies, which are not normally observed for samples prepared in the absence of organic peroxides. In the absence of clay, both DCP and DBP initiate de-acetylation and chain scission of EVA chains, but the influence of DBP is more pronounced. The presence of clay inhibits the initiation of EVA degradation by DCP free radicals, which can be observed in the higher tensile strength values for DCP treated samples, as well as in the de-acetylation step in the TGA curves. DBP has a more significant influence on the polymer degradation, and this gives rise to reduced thermal stability and mechanical properties. © 2008 Wiley Periodicals, Inc. J Appl Polym Sci 112: 218–225, 2009

Key words: EVA; Cloisite 15A clay; nanocomposites; morphology; thermal stability; tensile properties

INTRODUCTION

For many years inorganic fillers have been used to improve the performance of composite materials. Some of the popular inorganic fillers are alumina (α-Al_2O_3), calcium carbonate ($CaCO_3$), silica (SiO_2), feldspar ($KAlSi_3O_8$), and clay, especially montmorillonite. Montmorillonite is a soft phyllosilicate mineral that typically forms microscopic clay crystals. Chemically, it is a hydrated sodium calcium aluminum magnesium silicate hydroxide. The cations are replaced by ions bearing aliphatic chains so as to compatibilize the silicate, enhancing its interaction with the polymer by enlarging the interlayers. These modified silicates are known as organoclays.[1] These organoclays form intercalated, flocculated, or exfoliated morphologies in polymer nanocomposites, depending upon the delamination of the silicate layers, that provide exceptional properties such as increased modulus,[2,3] reduced gas permeability,[4,5] and enhanced thermal stability.[6–8]

Many polymer matrices have been investigated for developing polymer clay nanocomposites. Among these are vinyl polymers,[9,10] condensation step polymers,[11,12] polyolefins,[13,14] speciality polymers,[15,16] and biodegradable polymers.[17,18] Ethylene vinyl acetate (EVA) is a random copolymer which has a wide variety of applications such as cable insulating material, food packaging, thermoplastic elastomer, and drug delivery devices.[19–22]

The effect of ethylene glycidyl methacrylate (EGMA) and maleic anhydride grafted polypropylene (MAPP) on the structure and properties of EVA/Cloisite 15A clay nanocomposites have been investigated by Guduri and Luyt.[23,24] They found that EGMA strongly promotes clay exfoliation in the polymer matrix. However, the EGMA itself seemed to have a stronger influence on the thermal stability and tensile properties of the samples than the exfoliated clay. When MAPP was used as compatibilizer, there was not complete exfoliation of the clay, and the oxygen permeability was higher compared with samples containing EGMA as compatibilizer.

Crosslinking of a polymer matrix in composites and blends leads to an improvement in various material properties like Young's modulus.[25] Crosslinking is usually induced by thermal decomposition of an organic peroxide or by high energy irradiation, but less often by UV irradiation.[26] Recently, electron beam irradiation has been used for inducing crosslinking in EVA-clay nanocomposites.[27] It was reported that the crosslinking improved the various mechanical properties. It was found that especially the strength and thermal stability of the nanocomposites improved with an increase in irradiation dose.

In the present study, we prepared EVA/clay nanocomposites in the absence and presence of different organoperoxides. The aim was to initiate

Correspondence to: A. S. Luyt (luytas@qwa.uovs.ac.za).
Contract grant sponsor: National Research Foundation; contract grant number: ICD2006060100008.
Contract grant sponsor: University of the Free State in South Africa.

crosslinking to improve clay dispersion, which should give rise to improved thermal and mechanical properties. The samples were analyzed using XRD, SEM, TEM, TGA, and tensile testing.

EXPERIMENTAL

Materials

EVA copolymer with 9% vinyl acetate (VA) content was supplied by Plastamid, Elsies River, South Africa. The melting point of EVA was 95°C, and the density 0.930 g cm^{-3}.

Cloisite 15A clay (hydrogenated tallow ammonium salts of Bentonite), supplied by Southern Clay Products, Texas, USA, was used as reinforcement. The as received clay particles were disk-like stacks of thin silicate layers, 1 nm thick and ranging in length from 100 nm to several micrometers. The specific gravity of the clay particles (stacks), according to the suppliers, is 1.6–1.8 g cm^{-3}.

Dicumyl peroxide (DCP) and dibenzyl peroxide (DBP), used as crosslinking agents, were obtained from Aldrich Chemicals (WI, USA).

Preparation of nanocomposites

The EVA and organoclay were dried in an oven at 80°C overnight. They were melt blended using a Brabender Plastograph (Brabender, Duisberg, Germany) 50 mL mixer followed by extrusion using a Brabender Plastograph (Brabender, Duisberg, Germany) single screw extruder. 1, 2, and 3% by weight of clay were mixed with EVA for, respectively, 20 and 40 min at 130°C and 60 r.p.m. For peroxide cured samples, 1% DCP or DBP was added after the initial mixing, followed by 5 min mixing under the same conditions. The samples were then extruded at a screw speed of 60 r.p.m. at 130°C to obtain films with an average thickness of 0.45 ± 0.05 mm and an average width of 15 ± 1 mm.

Gel content determination

The gel content of the samples was determined using toluene as solvent. 1–2 g of each composite was wrapped in a stainless steel wire mesh (normal aperture 0.04 mm, wire diameter 0.04 mm) supplied by Meschcape Industries in Edenvale, South Africa, and refluxed in the solvent for 12 h, after which it was dried in an oven at 80 ± 5°C, followed by drying in air overnight. The gel content was determined as follows:

$$\text{Gel content} = (\text{mass of gel after solvent extraction} / \text{initial sample mass}) \times 100$$

X-ray diffraction analysis

The degree of intercalation or exfoliation was evaluated using X-ray diffractometry (XRD). X-ray diffraction patterns of the nanocomposite samples were obtained using a D8 Advance X-ray Diffractometer with CuK_α radiation, $\lambda = 1.5406$ Å (Bruker AXS Inc., Madison, WI, USA). Detector: Na-I scintillation counter with monochromator. The analyses were done in the reflection mode between $2\theta = 2°$ and 10°.

Tensile testing

A Hounsfield H5KS universal testing machine (Hounsfield, Redhill, England) was used to investigate the tensile strength, tensile modulus, and elongation properties of the nanocomposites. Samples of 150 mm × 15 mm × 0.45 mm were cut for tensile testing. Samples with a gauge length of 50 mm were analyzed at a crosshead speed of 10 mm min^{-1}. A continuous load-deflection curve was obtained. The averages and standard deviations of five tests per sample are reported.

Thermogravimetric analysis

Thermogravimetric analysis (TGA) was performed in a Perkin–Elmer TGA7 thermogravimetric analyser (Perkin–Elmer, Wellesley, MA). The sample mass was 6–8 mg. The analyses were carried out from 30 to 600°C at a heating rate of 10°C min^{-1} under nitrogen atmosphere (flow rate 20 mL min^{-1}).

Scanning electron microscopy

SEM analyses of the nanocomposites were performed using a JEOL WINSEM-6400 electron microscope (JEOL Ltd., Tokyo, Japan). The probe size was 114.98 nm, the probe current 0.02 nA, the noise reduction 64 Fr and the AC voltage 5.0 keV. The surfaces of the samples were coated with gold by an electrode deposition method to impart electrical conductivity before recording the SEM micrographs.

SEM-EDX (Energy Dispersive X-ray Diffraction)

The SEM-EDX analyses were done in a Shimadzu SSX-550 scanning electron microscope (Shimadzu Corp., Kyoto, Japan) at an AC voltage of 15.00 kV and a working distance of 17 mm. SEM-EDX pictures were taken from the same area as the SEM pictures.

Transmission electron microscopy

The samples were prepared using cryo-ultramicrotomy. They were mounted on cryo-pins and frozen in liquid nitrogen. Sections were cut at −100°C using a Reichert FCS (Leica, Vienna, Austria) attached to a Reichert Ultracut S Ultramicrotome. The sections

(100–150 nm thick) were collected on copper grids and viewed in a LEO 912 Omega (Carl Zeiss NTS GmbH, Oberkochen, Germany) TEM, with an energy filter, operating at 120 kV.

RESULTS AND DISCUSSION

In a previous article, we published results on EVA-Cloisite 93A nanocomposites prepared in the absence and presence of dicumyl peroxide (DCP) and dibenzoyl peroxide (DBP).[28] It was found that DCP and DBP had a different influence on the morphologies of the final products, and on the thermal and mechanical properties of the nanocomposites. In this study, we used the same preparation conditions, but a different organically modified clay, Cloisite 15A. The cations in Cloisite 93A and Cloisite 15A have slightly different structures, while the anions are HSO_4^- in the case of Cloisite 93A and Cl^- in the case of Cloisite 15A.

The TEM photo of EVA/clay (1%) prepared in the absence of organic peroxides [Fig. 1(a)] clearly shows that there was no intercalation or exfoliation of the clay layers in the polymer matrix, although the clay was fairly well dispersed in the polymer. This observation is in line with previous results.[23,24] For EVA/clay (1%) prepared in the presence of 1 phr DCP, the XRD spectra in Figure 1(b) show that this sample probably has a mixed morphology, with fairly weak (001) peaks at 2θ values lower than that of pure Cloisite 15A clay. This morphology is confirmed by the TEM photo in Figure 1(c), which shows a high level of clay delamination interspersed by intercalated clay tactoids. There is also strong orientation of the clay platelets in the draw direction. This must be the result of strong interaction between the matrix and the clay during sample preparation in the presence of DCP. Unfortunately, we could not do TEM analyses on EVA/clay (1%) samples prepared in the presence of DBP, but the XRD spectra in Figure 1(b) show that the sample premixed for 20 min has clay layers intercalated by polymer chains (decrease in 2θ value of peak maximum), with a possibility of partial exfoliation (decrease in peak intensity). It has, however, been shown that XRD is not a very reliable method for establishing clay intercalation/exfoliation at low clay contents,[29] and therefore the reference to partial exfoliation is purely speculative. The XRD spectrum of the sample premixed for 40 min shows no clay (001) peak, which is an indication of complete clay exfoliation in the EVA matrix. It is possible that the longer mixing time improved intercalation into the clay layers, which gave rise to complete delamination after the addition of DBP, significantly improved EVA-clay interaction.

For 2% clay containing samples the picture looks slightly different. The XRD spectra in Figure 2(a)

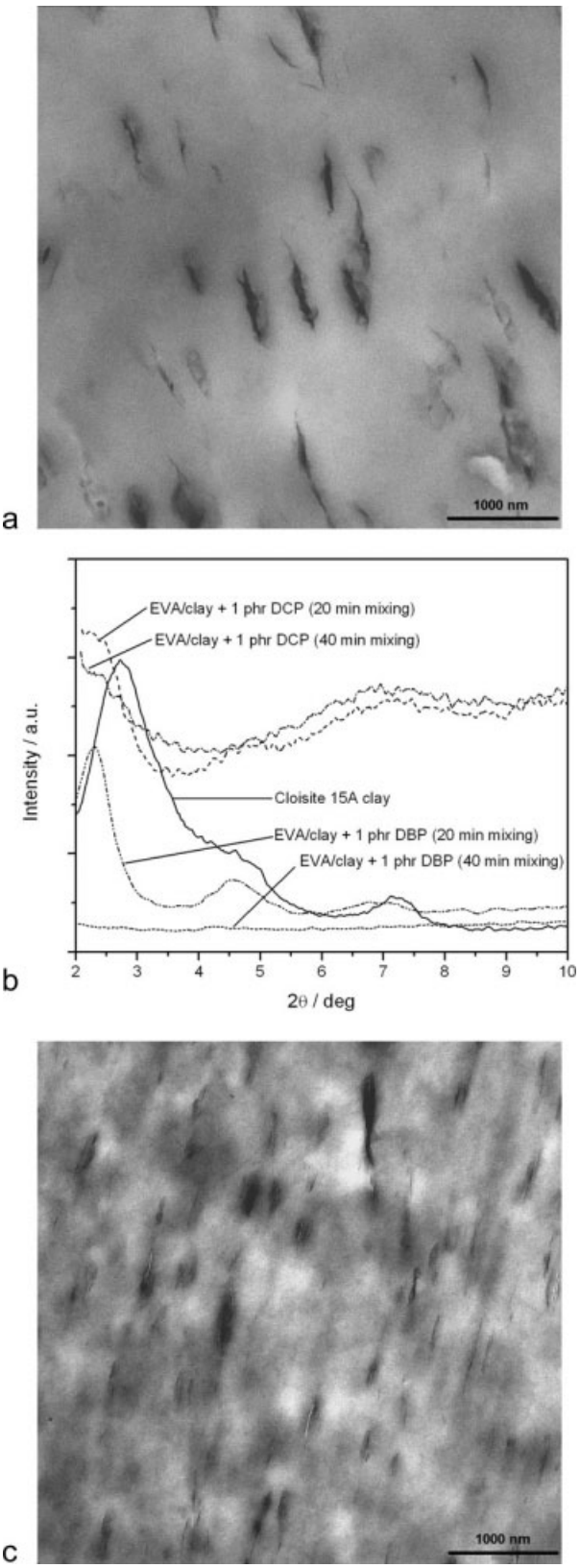

Figure 1 (a) TEM photo of 99/1 w/w EVA/clay, (b) XRD spectra of 1% clay containing samples, and (c) TEM photo of 99/1 w/w EVA/clay + 1 phr DCP.

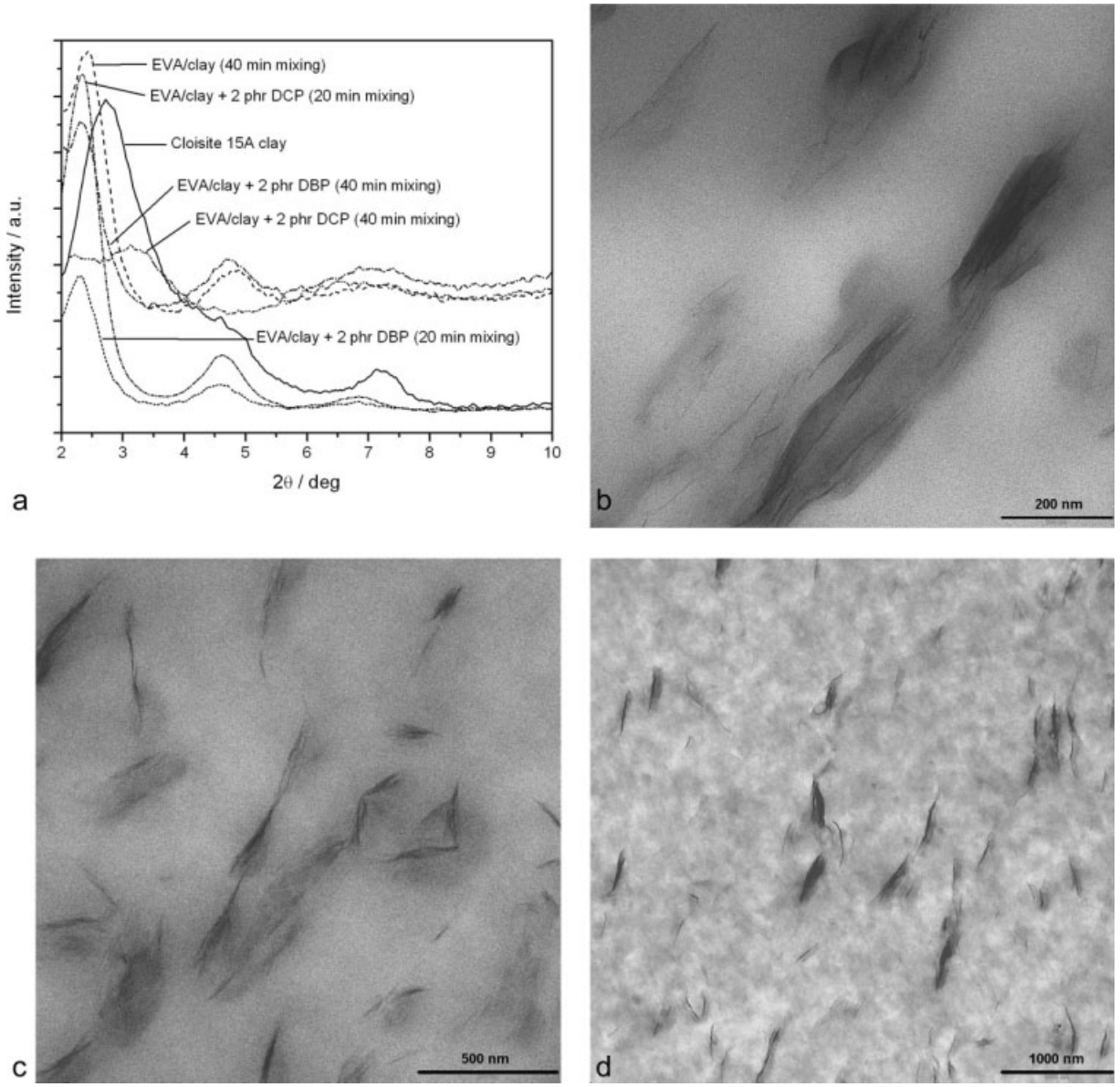

Figure 2 (a) XRD spectra of 2% clay containing samples, and TEM photos of (b) 98/2 w/w EVA/clay, (c) 98/2 w/w EVA/clay + 1 phr DBP, and (d) 98/2 w/w EVA/clay + 1 phr DCP.

show intercalated, exfoliated, and mixed morphologies. No direct relationship could be found between the observed morphology and the absence/presence and/or type of organic peroxide, as well as the initial mixing time. The TEM photos in Figure 2(b,c) clearly show the presence of an intercalated morphology, while Figure 2(d) shows a higher extent of exfoliation, in line with the XRD spectra. In the latter case, orientation in the draw direction is also observable. The XRD spectra for the EVA/clay (3%) samples in Figure 3 show mainly intercalation for samples prepared in the absence of peroxide and in the presence of DCP. For these samples the reduction in the values of 2θ is also less than in the case of the 1 and 2% clay containing samples. The samples prepared in the presence of DBP show a combination of intercalation and exfoliation, with a much larger *d*-spacing (smaller 2θ value) for the sample premixed for 40 min. It seems as if DBP generally has a stronger influence on EVA-clay interaction, probably because it is more decomposed under the sample preparation conditions. This is contrary to observations where we used Cloisite 93A as nanoclay. There we observed that DCP had a stronger influence, despite the fact that DCP has a much longer decomposition half-life under the preparation conditions.[28]

Scanning electron micrographs of EVA, EVA/clay without DCP and EVA/clay with DCP are shown in Figure 4. The SEM images show regular leaflet

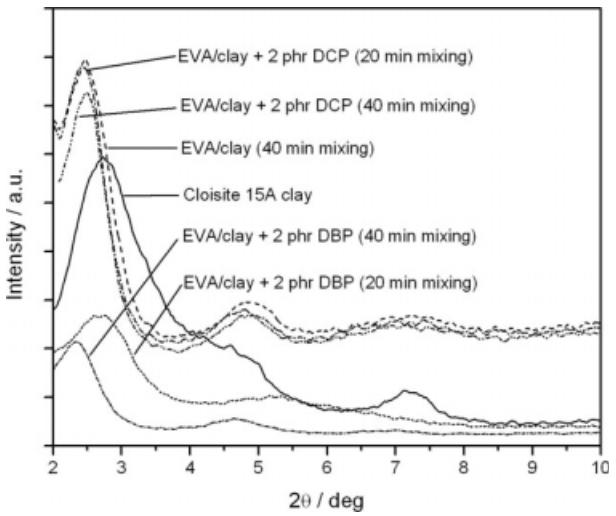

Figure 3 XRD spectra of 3% clay containing samples.

patterns for all the nanocomposite samples. We assume that the shear forces of the extrusion, combined with the attraction forces between the matrix and the clay, caused the clay layers to form this pattern. This assumption may be relevant if we compare Figure 4(a,b). Although the leaflet pattern is observed for the sample prepared in the absence of organic peroxide, it seems to be distorted and not so clearly defined as in the case of the sample prepared in the presence of 1 phr DBP. The DBP free radicals clearly improve the interaction between the clay platelets and the EVA chains, and this gives rise to the observed pattern. Gel contents for all the samples were determined through solvent extraction, but no

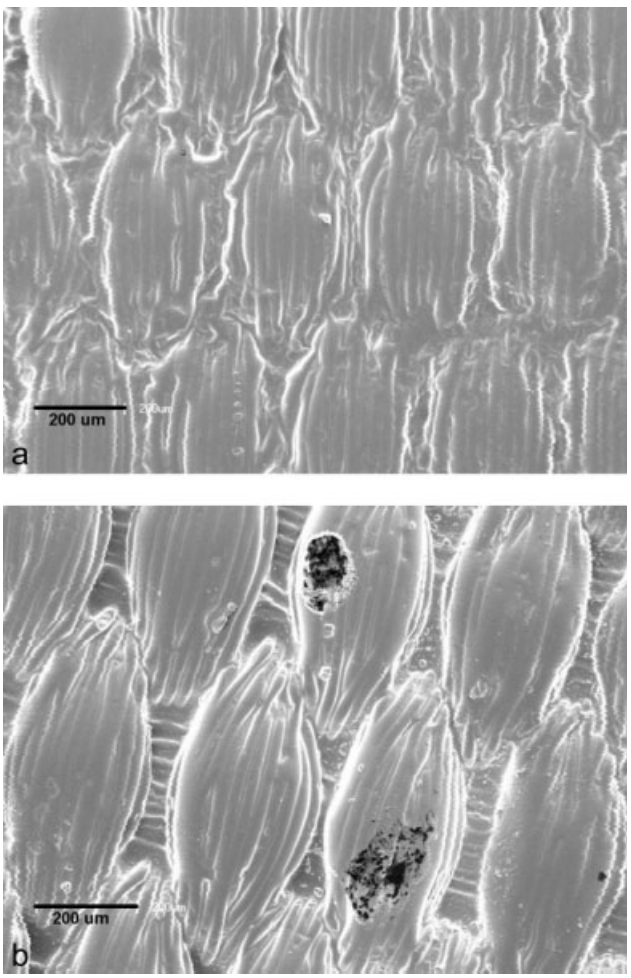

Figure 4 SEM photos of (a) 99/1 w/w EVA/clay and (b) 99/1 w/w EVA/clay + 1 phr DBP.

TABLE I
Tensile Results for all the Investigated Samples

Sample	$\sigma_b \pm s\sigma_b$ (MPa)	$\varepsilon_b \pm s\varepsilon_b$ (%)	$E \pm sE$ (MPa)
Pure EVA	6.5 ± 1.5	403 ± 87	24.8 ± 3.3
EVA/DCP	7.2 ± 0.3	700 ± 12[a]	10.3 ± 0.8[a]
EVA/DBP	6.0 ± 0.8	628 ± 70[a]	10.5 ± 0.6[a]
EVA/clay (1%) (40 min)	6.1 ± 0.1	383 ± 108	30.1 ± 1.7
EVA/clay (1%)/DCP (20 min)	8.6 ± 0.7	301 ± 16	40.0 ± 1.1
EVA/clay (1%)/DCP (40 min)	9.0 ± 0.5	381 ± 9	41.7 ± 3.0
EVA/clay (1%)/DBP (20 min)	6.6 ± 0.3	244 ± 37	23.5 ± 0.5
EVA/clay (1%)/DBP (40 min)	6.4 ± 0.3	279 ± 46	23.5 ± 1.1
EVA/clay (2%) (40 min)	7.4 ± 0.7	554 ± 89	44.6 ± 3.5
EVA/clay (2%)/DCP (20 min)	6.1 ± 0.3	226 ± 17	45.9 ± 2.3
EVA/clay (2%)/DCP (40 min)	7.7 ± 0.8	295 ± 21	39.9 ± 3.7
EVA/clay (2%)/DBP (20 min)	6.6 ± 0.7	249 ± 50	25.6 ± 2.0
EVA/clay (2%)/DBP (40 min)	6.4 ± 0.5	264 ± 75	24.3 ± 0.8
EVA/clay (3%) (40 min)	6.9 ± 0.4	465 ± 27	30.3 ± 4.0
EVA/clay (3%)/DCP (20 min)	8.1 ± 0.5	414 ± 17	33.4 ± 2.4
EVA/clay (3%)/DCP (40 min)	5.6 ± 1.0	137 ± 16	38.0 ± 1.6
EVA/clay (3%)/DBP (20 min)	6.6 ± 0.4	329 ± 57	23.6 ± 1.8
EVA/clay (3%)/DBP (40 min)	6.3 ± 0.3	152 ± 32	23.7 ± 2.4

σ_b, stress at break; ε_b, strain at break; E, Young's modulus; s, standard deviation.
[a] Young's modulus values are lower and strain at break values higher because extrusion conditions differed from those used for all the other samples.

TABLE II
Molecular Weight and Polydispersity Data of Pure EVA and EVA Prepared in the Presence of Respectively DCP and DBP

Sample	M_n	M_w	PD = M_w/M_n
EVA	5.25×10^4	2.97×10^5	5.7
EVA + 1 phr DCP	5.99×10^4	2.87×10^5	4.8
EVA + 1 phr DBP	5.61×10^4	2.72×10^5	4.9

gel formation was observed, and there was therefore no crosslink network formation. SEM-EDX analysis for Si shows a higher concentration of silica along the lines of the leaflet, but the photos are not clear enough to include in this article.

There are no substantial differences between the tensile strength values of the investigated samples (Table I). All the clay-containing samples, except those that were prepared in the presence of DCP, show tensile strength values in the same order as that of pure EVA. In the case of nanocomposites prepared in the absence of organic peroxide, the low clay contents and weak interaction between the EVA chains and Cloisite 15A clay explain the negligible influence on the tensile strengths of these samples. For the DBP treated samples, the increased interaction between the EVA and clay is probably balanced out by the degradation of EVA chains in the presence of DBP. The presence of such degradation is clear from the gel permeation chromatography (GPC) results presented in Table II. The GPC curve of pure EVA clearly shows a shoulder on the high-molecular weight side of the GPC curve, which is not visible in the curves of the peroxide treated EVA samples. Table II also shows a significant decrease in polydispersity for both peroxide treated samples. These observations clearly indicate chain scission in EVA in the presence of both DCP and DBP. However, the DCP treated clay-containing samples generally gave observably higher tensile strength values. Since DCP was used as crosslinking initiator at a temperature below its optimum decomposition temperature (1-h half-life at 136°C), while DBP was used at a temperature above its optimum decomposition temperature (1-h half-life at 91°C), it is possible that DCP only partially decomposed and that the available free radicals preferably reacted to improve the interaction between the clay and the EVA matrix, as already discussed in our previous article.[28] However, DBP would be completely decomposed under the preparation conditions, and enough free radicals would be available to initiate EVA-clay interaction as well as EVA chain scission. The tensile modulus values follow the same trends, and therefore the explanation of the differences between these values will be the same as for the tensile strengths.

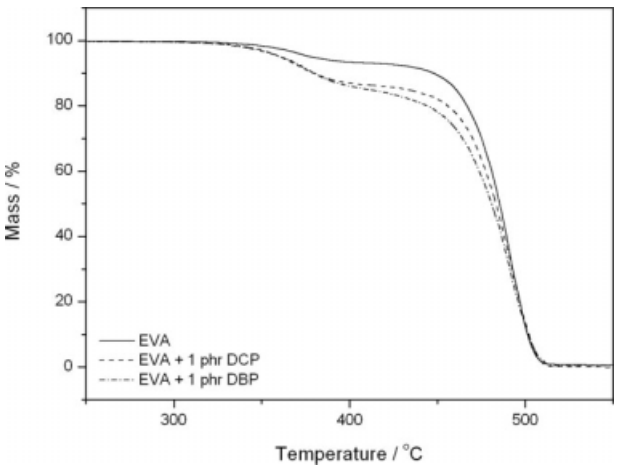

Figure 5 TGA curves of EVA samples prepared in the absence and presence of DCP and DBP.

The TGA curves (Figs. 5–8) show a two-step degradation for all the samples. The first step corresponds to the release of acetic acid, while thermal degradation of the ethylene-*co*-acetylene main chain takes place during the second step. Figure 5 shows that samples prepared in the presence of respectively, DCP and DBP have reduced thermal stability compared to pure EVA, with DBP having the largest degradative effect. This is the result of the degradation of EVA in the presence of organic peroxides, which is clear from the GPC results (Table II). Figures 6–8 show that pure EVA is generally more thermally stable than any of the nanocomposites, whether prepared in the absence or presence of peroxide. However, the effect on the de-acetylation step is less pronounced for DCP treated samples and for the samples prepared in the absence of peroxide. As already mentioned in the previous paragraph, DCP

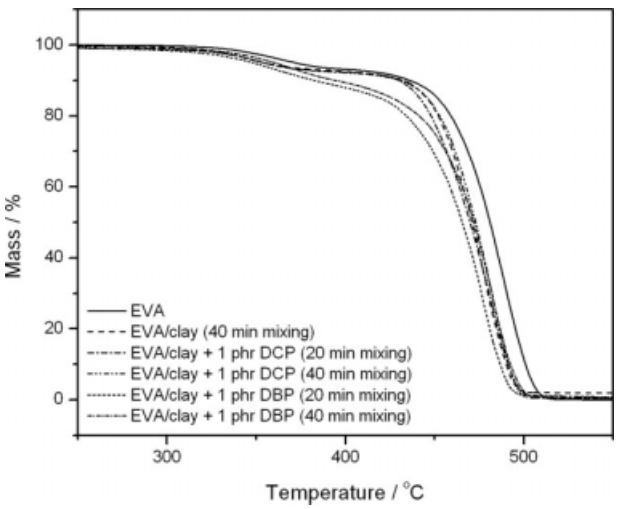

Figure 6 TGA curves of 1% clay containing samples.

in the presence of clay does not seem to effectively initiate chain scission and de-acetylation in EVA, probably because the available free radicals initiate some interaction between EVA and clay. DBP, on the other hand, is much more decomposed under the preparation conditions used in this study, and therefore there will be enough free radicals to also initiate chain scission and de-acetylation of EVA chains in DBP treated samples. The thermal decomposition of the organo-modifier in the clay may also generate acidic sites that will accelerate the de-acetylation of EVA in the nanocomposites, which should lead to accelerated backbone chain scission.[1] Figure 5 shows that for the DCP and DBP treated EVA samples, in the absence of clay, the second degradation step does not differ from that of pure EVA. However, this degradation occurs at observably lower temperatures for clay-containing samples.

CONCLUSIONS

The results in this article show that the presence of DCP or DBP during the preparation of EVA/Cloisite 15A clay nanocomposites gives rise to intercalated, exfoliated, or mixed morphologies, which are not normally observed for samples prepared in the absence of organic peroxides. In the absence of clay, both DCP and DBP initiate de-acetylation and chain scission of EVA chains, but the influence of DBP is more pronounced because of its complete decomposition under the preparation conditions. The presence of clay, however, inhibits the initiation of EVA degradation by DCP free radicals. The effect of this can be observed in the higher tensile strength values for DCP treated samples, as well as in the de-acetylation step in the TGA curves. DBP on the other hand, because of its complete decomposition under the preparation conditions, has a more significant influence on the polymer degradation, and this gives rise to reduced thermal stability and mechanical properties.

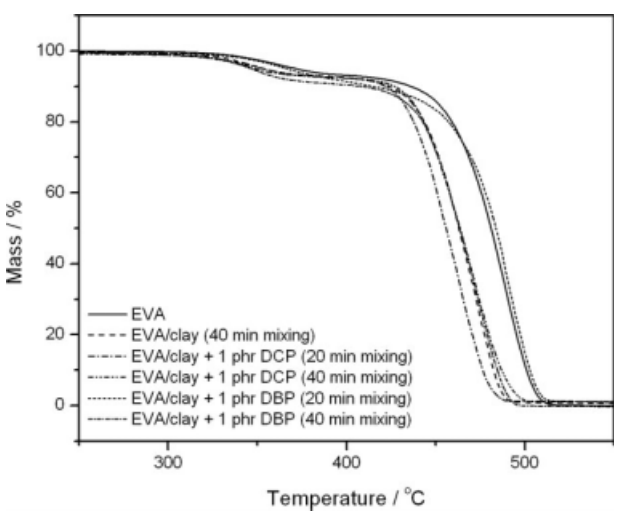

Figure 7 TGA curves of 2% clay containing samples.

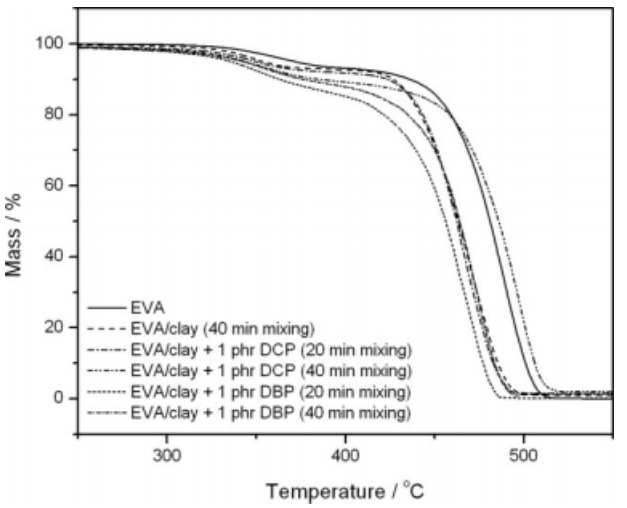

Figure 8 TGA curves of 3% clay containing samples.

Dr Remy Bucher from iThemba LABS in Somerset West, South Africa did the XRD analyses.

References

1. Zanneti, M.; Camino, G.; Thomann, R.; Mülhaupt, R. Polymer 2001, 42, 4501.
2. Vaia, R. A.; Price, G.; Ruth, P. N.; Ngumen, H. T.; Lichtenhan, J. Appl Clay Sci 1999, 15, 67.
3. Biswas, M.; Sinha Ray, S. Adv Polym Sci 2001, 155, 167.
4. Xu, R.; Manias, E.; Snyder, A. J.; Runt, J. Macromolecules 2001, 34, 337.
5. Zhu, J.; Morgan, A. B.; Lamelas, F. J.; Wilkie, C. A. Chem Mater 2001, 13, 3774.
6. Marriot, W. R.; Chen, E. Y.-X. J Am Chem Soc 2003, 125, 15726.
7. Garnweitner, G.; Smarsly, B.; Assink, R.; Ruland, W.; Bond, E.; Brinker, C. J. J Am Chem Soc 2003, 125, 5626.
8. Viville, P.; Lazzaroni, R.; Pollet, E.; Alexandre, M.; Dubois, P. J Am Chem Soc 2004, 126, 9007.
9. Zerda, A. S.; Caskey, T. C.; Lesser, A. J. Macromolecules 2003, 36, 1603.
10. Su, S.; Wilkie, C. A. J Polym Sci Part B: Polym Phys 2003, 41, 1124.
11. Morgan, A. B.; Gilman, J. W.; Jackson, C. L. Macromolecules 2001, 34, 2735.
12. Leu, C. M.; Wu, Z. W.; Wei, K. H. Chem Mater 2002, 14, 3016.
13. Usuki, A.; Tukigase, A.; Kato, M. Polymer 2002, 43, 2185.
14. Biswas, M.; Sinha Ray, S. Polymer 1998, 39, 6423.
15. Sinha Ray, S.; Biswas, M. J Appl Polym Sci 1999, 73, 2971.
16. Sinha Ray, S.; Okamoto, K.; Okamoto, M. Macromolecules 2003, 36, 2355.
17. Sinha Ray, S.; Yamada, K.; Okamoto, M.; Ogami, A.; Ueda, K. Chem Mater 2003, 15, 1456.
18. Duquesne, S.; Jama, C.; Bras, M. L.; Delobel, R.; Recourt, P.; Gloaguen, J. M. Comp Sci Technol 2003, 63, 1141.

19. Alexandre, M.; Beyer, G.; Henrist, C.; Cloots, R.; Rulmont, A.; Jerome, R.; Dubois, P. Macromol Rapid Commun 2001, 22, 643.
20. Maiti, P.; Yamada, K.; Okamoto, M.; Ueda, K.; Okamoto, K. Chem Mater 2002, 14, 4654.
21. Zhang, W.; Chen, D.; Zhao, Q.; Fang, Y. Polymer 2003, 44, 7953.
22. Cypes, S. H.; Saltzman, W. M.; Giannelis, E. P. J Controlled Release 2003, 90, 163.
23. Guduri, B. R.; Luyt, A. S. J Appl Polym Sci 2007, 103, 4095.
24. Guduri, B. R.; Luyt, A. S. J Appl Polym Sci 2007, 105, 3612.
25. Mičušík, M.; Omastová, M.; Nógellová, Z.; Fedorko, P.; Olejníková, K.; Trchová, M.; Chodák, I. Eur Polym Mater 2006, 42, 2379.
26. Lazar, M.; Rado, R.; Rychly, J. Adv Polym Sci 1990, 95, 149.
27. Sharif, J.; Dahlan, K. Z. N.; Yunus, W. M. D. W. Radiat Phys Chem 2007, 76, 1608.
28. Mishra, S. B.; Luyt, A. S. Express Polym Lett 2008, 2, 256.
29. Százdi, L.; Ábrányi, A.; Pukánszky, B., Jr.; Vansco, J. G.; Pukánszky, B. Macromol Mater Eng 2006, 291, 858.